

Dosimetric comparison of perineal and intra-vaginal interstitial template in image guided high dose rate brachytherapy for carcinoma cervix

V. Kaliyaperumal*, S. Banerjee, T. Kataria, S.K. Abraham, M. Veni S, S. Tamilselvan, D. Gupta, K. Dayanithi, D. Manigandan, S.R. Mishra, S.S. Bisht

Division Of Radiation Oncology, Medanta Cancer Institute, Medanta The Medicity, Gurgaon, Haryana, India

ABSTRACT

► Original article

*Corresponding author:

Venkatesan Kaliyaperumal, M.Sc.,

E-mail:

venkphysics@gmail.com

Received: December 2020

Final revised: December 2021

Accepted: December 2021

Int. J. Radiat. Res., July 2022;
20(3): 593-600

DOI: 10.52547/ijrr.20.3.11

Keywords: Image guided brachytherapy, optimization, intracavitary, interstitial, cervical cancer.

Background: The purpose of this study is to introduce a novel brachytherapy template called the Medanta anterior oblique-lateral oblique template (MAOLOT), which has been designed for carcinoma cervix, and conduct its dosimetric comparison with Martinez universal perineal interstitial template (MUPIT). **Materials and Methods:** Ten patients were chosen for this study with twelve intracavitary (IC) and/or interstitial (IS) applications. Plans were generated with basal points (BP), target points (TP), and inverse plan simulated annealing (IPSA) along with local graphical optimization (LGrO). Dosimetric and volumetric quantifiers including conformal index (COIN), dose non-uniformity ratio (DNR), dose homogeneity index (DHI), target dose homogeneity index (TDHI), and overdose volume index (OVI) were evaluated. **Results:** IPSA provided a better solution for DNR (range 0.25-0.48, $p=0.04$) in MUPIT and BP+LGrO method was appreciable ($p=0.08$) in OVI. Mean doses of D90, D95, and D98 of targets of LGrO plan were greater than their respective counterparts. Dose to 1cc and 2cc bladder was the highest for IPSA+LGrO plans as compared to forward optimization plans. Better COIN values were obtained for BP and TP plans with LGrO ($p=0.043$ (BP+LGrO), $p=0.022$ (TP+LGrO)). Mean EQD2 dose of 1cc and 2cc bladder was the highest for the IPSA plan as compared to other forward optimization plans. **Conclusion:** In IC+IS application, small adjustments using LGrO improves the target coverage and reduces the normal structure dose. IPSA provides better results if plan evaluation is performed carefully. MAOLOT creates the intracavitary and interstitial dose distribution, which is comparable to MUPIT.

INTRODUCTION

Cervical cancer is the fourth most frequent neoplastic diseases among women with high morbidity and mortality burden ⁽¹⁾. The intrinsic steep dose gradient of brachytherapy source allows a high dose to the tumor with relative sparing of the surrounding normal structures ⁽²⁾. Hence, radiation dose to the primary area is escalated with optimal clinical outcome and toxicities, and improved tumor control probability ⁽³⁾. Intracavitary radiotherapy (ICRT) is the conventional brachytherapy treatment for cancer cervix and one of the ICRT applicators is used with one central tandem and two ovoids with fixed loading patterns. It is comprised of intrauterine (tandem) and vaginal (ovoid/ring) sources. Dose distribution and non-anatomy-oriented Point A dosimetry does not provide favorable control rates ⁽⁴⁾ for large and irregular lesions in advanced cases, where the disease extends beyond the customary pear-shaped isodoses of conventional ICRT dose profile. There is a probability of underdosage to the

high-risk clinical target volume (HRCTV) if the applicator is not placed at the desired position, thereby increasing the HRCTV volume ⁽⁵⁾. Image guided brachytherapy (IGBT) in high-dose-rate (HDR) interstitial brachytherapy (ISBT) has the advantages of 3D volume dose prescription and reporting system.

Martinez universal perineal template (MUPIT) has the advantage of higher control for positioning the sources according to targets and organ at risks (OARs) with fixed geometry using needle template and obturator ⁽⁶⁾. MUPIT provides a better loco regional control for advanced gynecological malignancies in ISBT ⁽⁷⁾. Selection of the treatment plan is crucial in IGBT as it could provide better implants and clinical outcomes based on dose volume histogram (DVH) of targets and OARs. Optimization systems are different for interstitial and intracavitary brachytherapy like basal points (BP), target points (TP), inverse planning simulated annealing (IPSA), and local graphical optimization (LGrO). BP dose prescription of the Paris system provides an

adequate dosimetric coverage for the implanted volume ⁽⁸⁾. IPSA optimization significantly spares normal tissues without reducing target coverage, and the target conformity and homogeneity is superior in IPSA optimization when compared to LGrO ⁽⁹⁾. IPSA is a heuristic stochastic anatomy-based inverse optimization method. It optimizes the source-dwell position and it can provide user criteria based on input dose constraints with minimum and maximum dose constraints and penalty value. Dosimetric parameters are similar for inverse and manual optimization for improving the target coverage and for reducing the OAR dose ⁽¹⁰⁾. Volumetric GrO provides a better OAR sparing by increasing the homogeneity and conformity to the target ⁽¹¹⁾.

The primary aim of this study is to introduce a indigenously developed novel brachytherapy template called the Medanta anterior oblique-lateral oblique template (MAOLOT) for carcinoma (Ca) cervix in HDR brachytherapy and to compare with MUPIT for different dose optimization methods. MAOLOT has the provision to plan the conventional point A based plan as well as target volume based prescription. This template needs a initial dosimetric validation for Ca cervix patients with a clinically proven template (MUPIT) for further use in patients for all dosimetric optimization methods. Consequently, the study aims to compare the implant geometry and dose coverage between MAOLOT and MUPIT with the available planning methodology. This study also aims to compare the dose received by HRCTV, target dose volume indices, and OAR doses

for different methods of dose optimization for both templates. The treatment delivery time and total reference air kerma (TRAK) for both templates were correlated for the corresponding dose.

MATERIALS AND METHODS

Brachytherapy procedure and clinical plans

Ten patients with carcinoma cervix were chosen for the study with twelve interstitial applications (table 1). Informed consent was obtained from patients and the clinical implementation of MAOLOT template for patients was approved by the ethics committee of institutional review board (Ref No: MICR-980/2019). Five implants were done with MUPIT (Elekta Brachytherapy, Veenendaal, The Netherlands) and seven implants were done with MAOLOT; and all 12 implants were consecutively treated with computed tomography (CT)-based plans. Post-external beam radiotherapy (EBRT) MRI imaging was used to assess the residual disease and the number of needles required for implantation. The disease was again assessed during implantation by using the trans-rectal ultrasound probe. Urinary bladder was catheterized using 7ml of diluted radio opaque solution. The vaginal cylinder was inserted for MUPIT application after assessing the vaginal length. The MUPIT (figure 1a) was sutured to the perineum along with the cylinder in its position and the stainless-steel needles were inserted according to the geometry to be treated.

Table 1. patient demographics, number of needles and dose per fraction; Dose prescription provided for Brachytherapy after External beam Radiotherapy (45Gy/25F); AOLO-Anterior obliques lateral oblique; FIGO- International Federation of Gynecology and Obstetrics; HRCTV-High risk clinical target volume; SCC-Squamous cell carcinoma.

Template	Case No	Patient Demographics			No of Application	HRCTV Volume	No of Needles	Central Tandem	Dose Prescription
		Age	FIGO Staging	Histology					
MAOLT	1	63	IIIC	Adenocarcinoma	1	54.6	14	yes	6 Gyx2fraction
					2	78.5	14	yes	6 Gyx2fraction
	2	72	IIIB	SCC	1	100.2	18	yes	8 Gyx1fraction
					2	85.9	16	yes	8 Gyx2fraction
	3	72	IIB	SCC	1	101.2	19	yes	5.5 Gyx4fraction
MUPIT	4	56	IIB	SCC	1	67.5	18	yes	6.5 Gyx4fraction
	5	47	IIB	SCC	1	87.8	18	yes	7 Gyx4fraction
	6	76	IIIB	SCC	1	13.5	16	yes	4 Gyx4fraction
	7	58	IIIC	SCC	1	80.7	17	No	5 Gyx4fraction
	8	72	IIIA	SCC	1	100.8	21	No	4 Gyx8fraction
	9	56	IIIB	Adenocarcinoma	1	60.7	25	Yes	4.5 Gyx8fraction
	10	57	IIIB	SCC	1	64.6	17	Yes	6Gyx3fraction

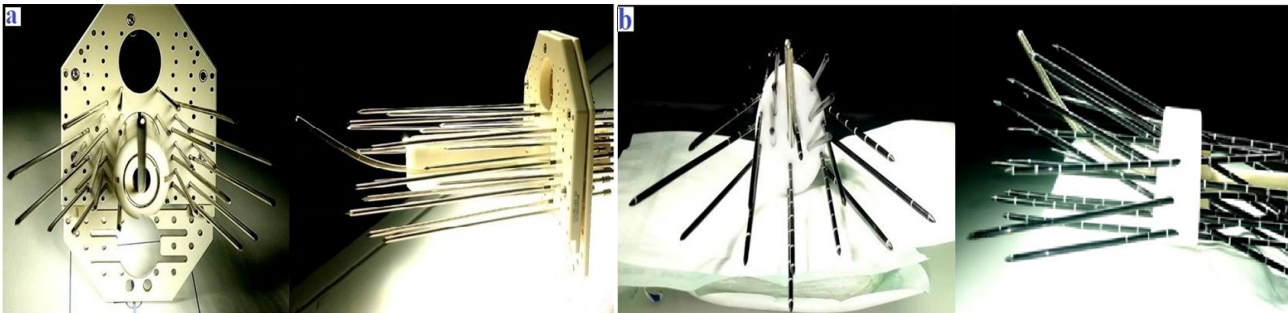


Figure 1. (a) schematic front and side view of MUPIT (Elekta medical system) with central tandem and lateral, straight needles. (b) schematic front and side view of MAOLOT with central tandem, anterior oblique, lateral oblique and straight needles; MAOLT -Medanta Anterior oblique lateral oblique template.

The MAOLOT is designed for the treatment of carcinoma cervix and it can effectively cover targets that extend laterally up to 4cm from the midline at the level of point A and the dosimetric validation of the MAOLOT was performed as per the standard protocol⁽¹²⁾. It can accommodate up to 19 needles (three anterior oblique, three lateral oblique and two straight needles on each side), thus resulting in 20 channels with the central tandem (figure 1b). In order to implant MAOLOT, the divergent needles and the number of needles were chosen with respect to the extent of the residual disease. As in the case of MUPIT application, all preliminary assessments were followed in this case too. Intra uterine tandem (Elekta Brachytherapy, Veenendaal, The Netherlands) was placed in the patient's uterine canal and the MAOLOT was inserted into the vaginal cavity. Anterior oblique and lateral oblique plastic needles (Kalyani Radiotherapy Specialty India Private Limited) were inserted through the cylinder. All patients underwent CT scans (Siemens SOMATOM Siemens Healthcare AG, Erlangen, Germany) with 2mm slice thickness after the implant. HRCTV and OAR like rectum, bladder, sigmoid and bowel were contoured as per the standard guidelines. All patients received EBRT with a dose ranging between 45Gy and 50Gy at 1.8-2Gy per fraction, followed by 4-6 fractions of ISBT.

Dosimetry and optimization

CT images were transferred to HDR Iridium-192 (micro selectron HDR, Elekta Brachytherapy, Veenendaal, The Netherlands) treatment planning system (TPS) (Oncentra master plan Version 4.5.3, Elekta Brachytherapy, Veenendaal, The Netherlands). HRCTV and OARs were delineated (figure 2) and dose calculations were performed using the American Association of Physicists (AAPM) task group-43 calculation methodology, after assuming a homogeneous water-equivalent geometry^(13,14). The needles were reconstructed using axial, sagittal, and coronal CT images and an 8mm offset was given for needles (as observed during the commissioning of applicator). The source was loaded according to the target geometry. The source-dwell position is defined either manually or automatically such that adequate target coverage is obtained.

Treatment plans were generated using forward and inverse optimization methods for both MUPIT and MAOLOT applications. The preliminary source loading for the MAOLOT was done in six anterior oblique needles (three needles on each side from the central tandem) to generate a point A-based dose distribution. The remaining source positions in the lateral oblique and straight needles were loaded with 10% to 20% (previously point A-based planned dwell time) using manual optimization to cover the entire target volume adequately⁽¹⁵⁾ (figure 3a). BP optimization was used to generate the base plan for

the MUPIT (figure 3b). Optimization methods with BP and TP along with local graphical optimization (LGrO) were followed in forward optimization. TP optimization is volume-based wherein the dose points are generated 5mm around the target surface and the dose is prescribed to these points. The central plane of the catheter points was created by using ECS and the basal dose points were placed by either visual inspection (manual) or tracking (automatic) in regular catheter geometry. Slight tailoring was performed with LGrO after the optimization of BP, TP, and IPSA to increase the target coverage and reduce the dose to normal structures. LGrO is a graphical tool where the planner can drag the isodose lines manually to either improve target coverage or spare OARs.

Dose equivalent to 2Gy (EQD_{2Gy}) calculation was performed to compute the dose to 90% of HRCTV and cumulative EQD_{2Gy} (including EBRT) of rectum and bladder. As per Groupe Européen de Curiethérapie and the European Society for Radiotherapy and Oncology (GEC-ESTRO) protocol, $D_{90\%}$ of HRCTV should get more than 85Gy, and D_{2cc} of rectum and bladder should be less than 75Gy and 90Gy, respectively⁽¹⁶⁾.

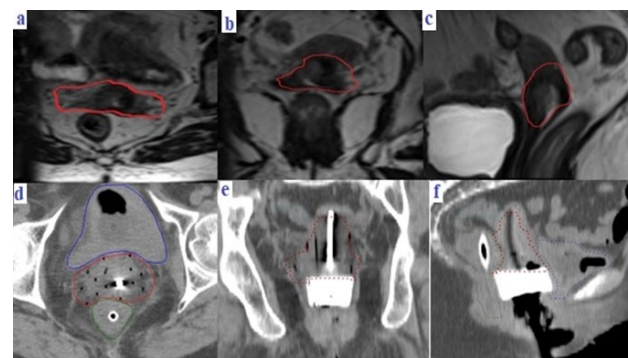


Figure 2. Delineation of HRCTV and normal structures by using pre-brachytherapy MRI in (a) axial view (b) coronal view (c) sagittal view and with applicator in CT scan (d) axial view (e) coronal view (f) sagittal view.

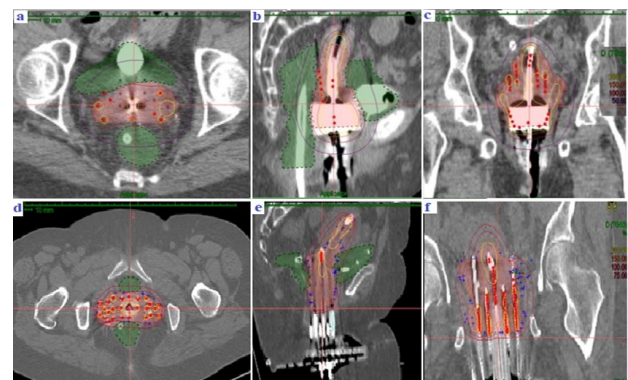


Figure 3. Dose distribution for Medanta AOLO application with (a) axial, (b) coronal and (c) sagittal section of CT images shows the target point optimization with manual local graphical optimization. Dose distribution for MUPIT application with (d) axial, (e) coronal and (f) sagittal section shows the basal dose point optimization with manual local graphical optimization.

Plan evaluation

Dosimetric outcomes of all plans generated with forward and inverse optimizations were analyzed quantitatively and qualitatively by using Dose Volume Histogram (DVH) parameters. The target dose parameters included $V_{100\%}$, $V_{150\%}$, and $V_{200\%}$ (target volume receiving 100%, 150%, and 200%, respectively, of the prescribed dose of radiation), and dose to 2cc volume of bladder and rectum for each plan. Other volumetric quantifiers including conformal index (COIN), dose non-uniformity ratio (DNR), dose homogeneity index (DHI), target dose homogeneity index (TDHI), and overdose volume index (OVI) were also evaluated⁽¹⁷⁾. COIN, equation 1, describes how well the prescribed dose encompasses the target volume and excludes non-target structures.

$$\text{Conformal index (COIN)} = \frac{\text{PTV PD} \times \text{PTV PD}}{V \text{ PTV} \times V \text{ PD}} \quad (1)$$

PTV PD = target volume receiving prescribed dose; V PTV = target volume; V PD = volume receiving prescribed dose

Dose non-uniformity ratio, equation 2, is defined as the ratio between the target volume that receives a dose equal to or greater than 1.5 times of the reference dose ($V_{1.5 \text{ ref}}$) and the target volume that receives a dose equal to the reference (prescribed) dose ($V \text{ ref}$).

$$\text{Dose non-uniformity ratio (DNR)} = \frac{V_{1.5 \text{ ref}}}{V \text{ ref}} \quad (2)$$

DHI, equation 3, is defined as the ratio between the fraction of target volume receiving a dose in the range of 1.0 to 1.5 times of the reference dose to the volume of the target that receives a dose equal to or greater than the reference dose.

$$\text{Dose homogeneity index (DHI)} = \frac{V_{\text{ref}} - V_{1.5 \text{ ref}}}{V \text{ ref}} \quad (3)$$

TDHI, equation 4, is defined as the ratio of fraction of target volume that receives a dose equal to or more than 1.5 times of reference (prescribed) dose to the volume of the target that receives a dose equal to or greater than the reference (prescribed) dose.

$$\text{Target dose homogeneity index (TDHI)} = \frac{V_{100} - V_{150}}{V_{150}} \quad (4)$$

OVI, equation 5, is defined as the ratio between the volume receiving twice the prescription dose and the volume of PTV. The doses to HRCTV and OAR were calculated by combining the EBRT and BT doses and by using the Linear Quadratic (LQ) dose effect model. The α/β value was taken as 10Gy and 3Gy for the target and OAR, respectively.

$$\text{Overdose volume index (OVI)} = \frac{V_{2 \text{ PD}}}{V \text{ PTV}} \quad (5)$$

Statistical analysis

Non-parametric related sample Wilcoxon Signed

Ranks Test was used for analyzing the dosimetric indices. EQD_{2Gy} of HRCTV, bladder, rectum, sigmoid, and bowel doses between MAOLOT and MUPIT was analyzed by using paired sample student *t-test*, which analyzes two sets of paired data's variation and estimates the probability (p value) whether the hypothesis "no difference between the two data sets" is true. It is acceptable if the p value is $0 < 0.05$, which indicates that the difference between the compared data sets is statistically significant. All statistical analyses were done with IBM SPSS Statistics for Windows, version 24 (IBM Corp., Armonk, NY, USA).

RESULTS

Dosimetric indices

For MUPIT, IPSA provided a better solution in the range of 0.25-0.48 ($p=0.04$) for DNR and it provided a better solution in the range of 0.29-0.44 ($p=0.043$) for IPSA+LGrO. IPSA provided better DHI in the range of 0.52-0.75 ($p=0.033$). No significant difference was found in TDHI and COIN when compared with various optimizations. The BP+LGrO method gave better OVI values ($p=0.08$) than other methods (table 2). For MAOLOT, no significant deviation was found in DNR, DHI, and OVI among various optimizations. TP optimization and TP+LGrO rendered significantly better values for TDHI in the range of 0.46-0.93 ($p=0.041$) and 0.50-0.93 ($p=0.009$), respectively, when compared to other methods. Better COIN values were obtained for basal point and target point plans with graphical optimization ($p=0.043$ (BP+LGrO), $p=0.022$ (TP+LGrO)), when compared to other methods (table 3).

Target dose

In MUPIT, volume of target receiving 200% dose ($V_{200\%}$) ranged from 16.9cc to 19.5cc for different optimization techniques with the IPSA optimization having the lowest value of 16cc. In MAOLOT, mean of $V_{200\%}$ ranged from 15.5cc to 25.6cc for different optimization methods. $V_{100\%}$ was almost the same for all optimization plans within the range of 115cc-117 cc, except for the BP plan, which had a lower value of 107cc (table 4). In the case of BP+LGrO optimization for MUPIT, HRCTV D90 and D95 values were 73.30Gy and 70.75Gy, respectively. BP+LGrO and IPSA+LGrO provided better results when compared with other methods. Mean doses of D90, D95, and D98 of target of LGrO plans were greater than their respective counterparts without LGrO for both forward and inverse optimization plans, while respecting the OAR doses. TP with LGrO provided better results for MAOLOT applicator when compared to other plans. The highest target dose was received by the IPSA+LGrO plan with mean values of D90, D95, and D98 being 83.44Gy, 78.89Gy, and 74.74Gy, respectively, which was comparable to the coverage achieved in the MUPIT application (figure 4).

Table 2. comparison of dosimetric indices with different optimization techniques for MUPIT (p value derived by using related sample wilcoxn signed rank test); BP+GrO- Basal point+Graphical optimization; TP-Target points; TP+GrO- target points+Graphical optimization; IPSA-Inverse planning simulated annealing; IPSA+GrO- Inverse planning simulated annealing+Graphical optimization.

MUPIT	BP+GrO		TP		TP+GrO		IPSA		IPSA+GrO	p
	Range	p	Range	p	Range	p	Range	p		
DNR	0.39-0.49	0.893	0.38-0.54	0.225	0.36-0.53	0.203	0.25-0.48	0.04	0.29-0.44	0.043
DHI	0.49-0.63	0.893	0.46-0.61	0.225	0.47-0.64	0.198	0.52-0.75	0.033	0.56-0.71	0.138
TDHI	0.43-0.69	0.5	0.47-0.74	0.138	0.44-0.66	0.215	0.41-0.75	0.225	0.44-0.71	0.5
OVI	0.15-0.27	0.08	0.14-0.23	0.345	0.16-0.25	0.311	0.07-0.14	0.043	0.09-0.20	0.5
COIN	0.78-0.88	0.5	0.78-0.96	0.686	0.80-0.86	0.582	0.72-0.84	0.08	0.65-0.86	0.225

Table 3. Comparison of dosimetric indices with different optimization techniques for Medanta AOLO (p value derived by using related sample wilcoxn signed rank test) BP+GrO- Basal point+Graphical optimization; TP-Target points; TP+GrO- target points+Graphical optimization; IPSA-Inverse planning simulated annealing; IPSA+GrO- Inverse planning simulated annealing+Graphical optimization.

Medanta AOLO	BP+GrO		TP		TP+GrO		IPSA		IPSA+GrO	
	Range	p	Range	p	Range	p	Range	p	Range	p
DNR	0.44-0.53	0.225	0.45-0.48	0.345	0.46-0.50	0.115	0.40-0.53	0.225	0.41-0.49	0.138
DHI	0.48-0.59	0.416	0.52-0.55	0.345	0.51-0.54	0.181	0.47-0.66	0.893	0.51-0.58	0.138
TDHI	0.52-0.89	0.138	0.46-0.93	0.041	0.50-0.98	0.009	0.40-0.60	0.500	0.41-0.78	0.500
OVI	0.21-0.26	0.273	0.19-0.23	0.500	0.21-0.27	0.112	0.15-0.27	0.686	0.14-0.27	0.465
COIN	0.73-0.82	0.043	0.78-0.84	0.044	0.79-0.84	0.022	0.67-0.74	0.500	0.69-0.74	0.500

Table 4. different dosimetric parameters of HRCTV for MUPIT and MAOLO; MUPIT- Martinez universal perineal interstitial template; BP-Basal points; MAOLO- Medanta anterior oblique lateral oblique template; BP+GrO- Basal point+Graphical optimization; TP-Target points; TP+GrO- target points+Graphical optimization; IPSA-Inverse planning simulated annealing; IPSA+GrO- Inverse planning simulated annealing+Graphical optimization.

HRCTV		BP	BP+LGRO	TP	TP+LGRO	IPSA	IPSA+LGRO
MUPIT	V200%(cc)	16.9	18.3	19.4	19.5	16	17.6
	V150%(cc)	36.5	40.7	40.7	40.9	40.4	42.2
	V100%(cc)	70.1	73.3	73.3	74.4	73.4	76.8
MAOLO	V200%(cc)	15.5	22	23.9	24.8	25.6	19.7
	V150%(cc)	45.5	56.5	59.7	55.9	56.8	51.6
	V100%(cc)	107	116	115	116	115	117

OAR dose

In MUPIT cases, a range of volumes (1cc and 2cc) was analyzed for comparing bladder and rectum doses. Mean EQD2 dose of 1cc and 2cc bladder was the highest for the IPSA+LGrO plan with values 79.66Gy and 75.44Gy, respectively, as compared to other forward optimization plans. In MAOLO, mean EQD2 dose of 1cc and 2cc bladder was the highest for the IPSA plan with values 82.57Gy and 78.44Gy, respectively, as compared to other forward optimization plans. In MUPIT, mean dose of 1cc and 2cc rectum was found to be the highest in the TP plan with values 71.97Gy and 69.32Gy, respectively. In MAOLO, the lowest mean dose of 1cc and 2cc rectum was found to be for the IPSA+LGrO plan with values 74.27Gy and 70.91Gy, respectively (figure 5). The lower bladder and rectum doses attribute to the steep dose fall-off outside the prescription isodose, wherein the LGrO plays a significant role. In MUPIT, the mean EQD2Gy(3) received by 1cc bowel and 2cc bowel was within 65Gy and 60Gy, respectively, for all optimizations. In Medanta AOLO, EQD2Gy(3) received by 1cc bowel and 2cc bowel was within

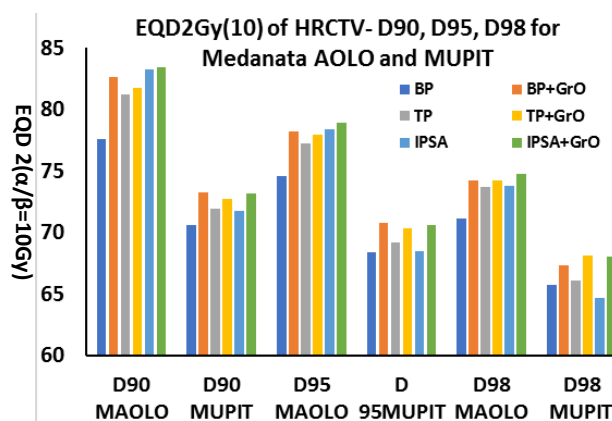


Figure 4. Mean EQD2 ($\alpha/\beta=10$ Gy) value for HRCTV with different type of optimization methods –Medanta AOLO and MUPIT. EQD2-Equivalent dose to 2Gy (including EBRT); D90- EQD2 of dose received by 90% of HRCTV volume; D95- EQD2 of dose received by 95% of HRCTV volume; D98- EQD2 of dose received by 98% of HRCTV volume; BP-Basal points; MAOLO- Medanta anterior oblique lateral oblique; BP+GrO- Basal point+Graphical optimization; TP-Target points; TP+GrO- target points+Graphical optimization; IPSA-Inverse planning simulated annealing; IPSA+GrO- Inverse planning simulated annealing+Graphical optimization.

65Gy and 60Gy, respectively, for all optimizations. In MUPIT, Sigmoid 1cc and Sigmoid 2cc received doses within 70Gy and 65Gy, respectively, for all optimizations. In MAOLO, sigmoid received higher mean doses when compared to MUPIT for all optimizations. Sigmoid 1cc mean doses were in the range of 77-70Gy and sigmoid 2cc mean doses were in the range of 72-67Gy, and these were the lowest for the IPSA+LGrO optimization (figure 6).

Delivery parameters

In MUPIT, the difference regarding the treatment delivery time was minimal in forward and inverse optimization plans. In view of total reference air

kerma (TRAK), IPSA+LGrO had a comparatively high value than other optimizing modalities. Basal point optimization had less TRAK values than other optimizations. In MAOLOT, the TRAK values, which represent the integral dose to patients, were also a parameter to assess the treatment plan. An optimum TRAK per fraction per pulse value (<0.5) was achievable in all cases, which qualified the plan deliverability. Comparison of treatment time among optimization techniques did not show a significant difference (figure 7).

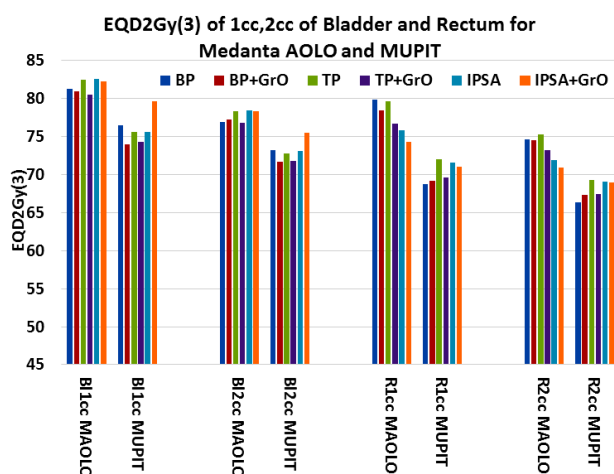


Figure 5. Mean EQD2 ($\alpha/\beta=3\text{Gy}$) value of 1cc, 2cc of Bladder and rectum with different type of optimization methods – Medanta AOLO and MUPIT. EQD2-Equivalent dose to 2Gy (including EBRT); BI1cc-1cc of bladder volume receiving EQD2Gy; BI2cc-2cc of bladder volume receiving EQD2Gy; RLcc-1cc of rectum volume receiving EQD2Gy; R2cc-2cc of rectum volume receiving EQD2Gy.

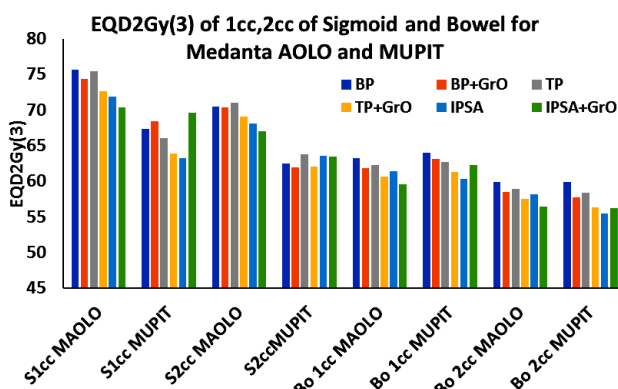


Figure 6. Mean EQD2Gy($\alpha/\beta=3\text{Gy}$) value of 1cc, 2cc of Sigmoid and Bowel with different type of optimization methods – Medanta AOLO and MUPIT; EQD2-Equivalent dose to 2Gy (including EBRT); S1cc-1cc of sigmoid volume receiving EQD2Gy; S2cc-2cc of sigmoid volume receiving EQD2Gy; Bo1cc-1cc of bowel volume receiving EQD2Gy; B2cc-2cc of bowel volume receiving EQD2Gy.

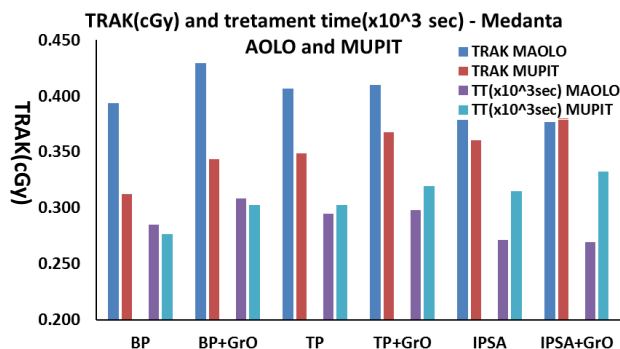


Figure 7. TRAK (cGy) and treatment time for various optimization methods in MAOLOT and MUPIT; TRAK- total reference air kerma in cGy; TT-treatment time in seconds.

DISCUSSION

Different optimization methods were used to compare the preliminary dosimetric studies between the perineal template and the indigenously developed intracavitary with interstitial template. Several authors have reported different range of dosimetric indices for the interstitial Brachytherapy. Study by Major *et al.* ⁽¹⁸⁾ using ideal double plane hypothetical implants reported values of 0.82 for COIN and 0.68 for DHI. Our conformity values are in the range 0.69-0.86 for MAOLOT and 0.67-0.84 for MUPIT. These values are similar to the earlier study done by Sharma *et al.* ⁽⁸⁾ in using MUPIT with COIN values in range 0.71-0.85 (mean 0.79 ± 0.05) and stated that BP with LGrO could satisfy the target coverage without increasing the OAR doses in gynecological image based interstitial brachytherapy. They also studied optimization methods and stated that BP with LGrO could satisfy the target coverage without increasing the OAR doses. Jamema *et al.* ⁽⁹⁾ compared IPSA and manual optimization and have shown the superiority of IPSA optimisation compared to manual and basal point optimisation for most of the dosimetric indices except DHI, but in some cases manual optimization was clinically acceptable because inverse planning produces unacceptably high dose regions near the needles, when compared with manual plans. In the present study, IPSA alone did not provide the adequate target coverage and reduce the dose to OAR. However, IPSA with LGrO provided a desirable dose distribution (without increasing the high dose regions) along with reduced OAR doses for both MAOLOT and MUPIT. Fröhlich *et al.* analyzed the dosimetric comparison between inverse and forward optimization methods and concluded that inverse plans were of lesser quality in terms of homogeneity and such plans generally resulted in a longer active length than necessary in clinical cases ⁽¹⁹⁾. In another study, Jamema *et al.* ⁽²⁰⁾ stated that IPSA provided a significant reduction in the normal structure dose than manual optimization without compromising

target coverage, wherein careful clinical validation was also needed.

Shwetha *et al.* ⁽¹¹⁾ studied the dosimetric comparison of various optimization techniques for interstitial cervix implants and stated that TP optimization was the simplest method to cover HRCTV; but it prioritized target coverage instead of regulating normal structure doses, which were delivered to nearby targets like the rectum, bladder, and sigmoid. Further, high dose region among the more spaced needles could not be eliminated. In our study, due to applicator geometry and needle placement, TP optimization was not adequate to cover the target for MUPIT and MAOLOT and it deteriorated the conformity and homogeneity of the target. LGrO was incorporated with TP optimization to increase the target coverage and homogeneity.

In the present study, MUPIT and MAOLOT were used in cervical cancer, which require target coverage up to 5cm beyond midline in all directions. Based on the results, it is inferred that BP with LGrO provides better dosimetric results if the target volume is lesser than the implant geometry ⁽⁸⁾. Chakrabarti *et al.* compared dose volume parameters using forward planning techniques involving two applicators and concluded that forward optimization methods provide a manual intervention to control and eliminate undesirable distributions in the inverse planning process ⁽²⁰⁾. In the present study findings, mean central dose (MCD) was the mean dose of BP and it was considered for normalization of the prescription dose. Although a homogenous dose distribution could be obtained, target coverage and conformity were not appreciable for both MUPIT and MAOLOT. LGrO occasionally led to unpredictable changes in dwell times and subsequently increased the high dose or low dose regions in the implant geometry, if the needles were not placed perfectly in HRCTV.

Some authors studied about inverse planning applications and compared them with forward optimization methods. Jamema *et al.* stated that IPSA provided good conformity and target homogeneity in ISBT without reducing the target coverage, while comparing the dose point and manual optimization but IPSA provided a significant reduction in the normal structure dose without compromising target coverage, when compared to manual optimization wherein careful clinical validation was needed ⁽²¹⁾. IPSA can provide superior results, if the needles are uniformly placed and the distance between the needles is maintained within the target volume. IPSA can lead to unrealistic dwell times in non-uniform geometries, causing either an underdose or an overdose, and this dose distribution was modified and improved by using LGrO based on target volume ^(22, 23). Kumar *et al.* discussed the dose fractionation schemes and its effects on critical structures like bladder and rectum. The EQD2 of normal structures

and dose to 90% of HR CTV remains same for the different dose fractionation schedule such as 5.5 Gy × 5 fractions, 6.5 Gy × 4 fractions, and 7 Gy × 4 fractions ⁽²⁴⁾. In our study, the dose fractionation schemes were chosen based on the EQD2 of target and normal structures. The average of maximum EQD2 for the 2cc of bladder and rectum was 87.56 and 74.57 Gy respectively in manual with local graphical optimization method. This method could be used in efficient way to reduce the critical structure dose as well as improving the target EQD2.

In the present study, inverse planning optimizers like IPSA with LrGO allowed potentially high dose escalation, provided the dose coverage was adequate and dose to OAR was minimized. LGrO with TP optimization reduced the dose to rectum, bladder, and sigmoid, but it led to an increase or decrease in the dwell time near the target boundary. The present study shows non-inferiority of the interstitial template with the standard perineal one. Thus, MAOLOT has the advantage of pear shape dose distribution with similar or better dosimetric results and it also has an operational advantage. In future work, MAOLOT could be compared with commercially available templates or applicators for further validation.

CONCLUSION

In the present study, forward optimization with careful usage of LGrO provided a visual tool for shaping the dose distribution to improve target coverage and reduce dose to both rectum and bladder. This method produced higher target coverage (4-7%) without changing the dosimetric indices (COIN, DNR, DHI, TDHI, OVI) and dose to OARs. In the IC+IS application, slight adjustments made by using LGrO could improve the target coverage and reduce the normal structure dose. IPSA provided better results, if plan evaluation was performed carefully. Regarding the applicators' geometry, the MAOLOT could create the intracavitary and interstitial dose distributions, which were comparable to MUPIT.

ACKNOWLEDGEMENTS

The author wishes to thank Mr. Christy Alekchander, Chief Medical Physicist, Patel Hospital, Jalandar, Punjab for providing technical feedback.

Funding: This research received no grant from any funding agency in the public, commercial, or not-for-profit sectors.

Ethics approval and consent to participate: Medanta AOLO Brachytherapy template is approved by Ethics committee of institutional review board for the clinical applications (Ref No: MICR-980/2019).

Author contributions: Data Data curation: VK, SB,

TK, SKA, MV, ST, DG, KD, DM, SRM, SSB. Data analysis: VK, SB, TK, SKA, SRM. Funding acquisition: No fund is received. Investigation: VK, SB, TK, ST, DG, SSB. Writing-original draft: VK, SB, TK, SKA. Writing-English translation: VK, SB, TK, SKA, MV, ST, DG, KD, DM, SRM, SSB.

Conflicts of interest: Declared none.

REFERENCES

1. Torre LA, Islami F, Siegel RL, Ward EM, Jemal A (2017) Global cancer in women: Burden and Trends. *Cancer Epidemiol Biomarkers Prev*, **26**(4): 444-457.
2. Cihoric N, Tsikkinis A, Tapia C, Aebbersold DM, Zlobec I, Lössl K (2015) Dose escalated intensity modulated radiotherapy in the treatment of cervical cancer. *Radiat Oncol*, **24**(10): 240.
3. Baltas D (2006) The physics of modern brachytherapy for oncology. 1st ed. New York: Taylor & Francis.
4. Murakami N, Kobayashi K, Kato T, Nakamura S, Wakita A, Okamoto H, et al. (2016) The role of interstitial brachytherapy in the management of primary radiation therapy for uterine cervical cancer. *J Contemp Brachytherapy*, **8**(5): 391-398.
5. Goyal MK, Rai DV, Manjhi J, Barker JL, Heintz BH, Shide KL, et al. (2017) Study of dosimetric and spatial variations due to applicator positioning during inter-fraction high-dose rate brachytherapy in the treatment of carcinoma of the cervix: A three dimensional dosimetric analysis. *Int J Radiat Res*, **15**(4): 377-382.
6. Martinez A, Cox RS, Edmundson GK (1984) A multiple-site perineal applicator (MUPIT) for treatment of prostatic, anorectal, and gynecologic malignancies. *Int J Radiat Oncol Biol Phys*, **10**(2): 297-305.
7. Nandwani PK, Vyas RK, Neema JP, Suryanarayan UK, Bhavsar DC, Jani KR (2007) Retrospective analysis of role of interstitial brachytherapy using template (MUPIT) in locally advanced gynecological malignancies. *J Cancer Res Ther*, **3**(2): 111-5.
8. Sharma PK, Swamidas JV, Mahantshetty U, Deshpande DD, Manjhi J, Rai DV (2014) Dose optimization in gynecological 3D image based interstitial brachytherapy using martinez universal perineal interstitial template (MUPIT) -an institutional experience. *J Med Phys*, **39**(3): 197-202.
9. Jamema SV, Sharma S, Mahantshetty U, Engineer R, Shrivastava SK, Deshpande DD (2011) Comparison of IPSA with dose-point optimization and manual optimization for interstitial template brachytherapy for gynecologic cancers. *Brachytherapy*, **10**(4): 306-12.
10. Palled SR, Radhakrishna NK, Manikantan S, Khanum H, Venugopal BK, Vishwanath L (2020) Dosimetric comparison of manual forward planning with uniform dwell times versus volume-based inverse planning in interstitial brachytherapy of cervical malignancies. *Rep Pract Oncol Radiother*, **25**(6): 851-855.
11. Shwetha B, Ravikumar M, Katke A, Supe SS, Venkatagiri G, Ramnand N, et al. (2010) Dosimetric comparison of various optimization techniques for high dose rate brachytherapy of interstitial cervix implants. *J Appl Clin Med Phys*, **11**(3): 3227.
12. Banerjee S, Kaliyaperumal V, Kataria T, Kamaraj D (2022) The Medanta AOLO template for locally advanced cancer cervix brachytherapy: design and clinical implementation. *J Contemp Brachytherapy*, **12**(1): 44-47.
13. Meigooni AS (2004) Recent developments in brachytherapy source dosimetry. *Int J Radiat Res*, **2**(3): 97-105.
14. Rivard MJ, Coursey BM, DeWerd LA, Hanson WF, Huq MS, Ibbott GS, et al. (2004) Update of AAPM Task Group No. 43 Report: A revised AAPM protocol for brachytherapy dose calculations. *Med Phys*, **31**(3): 633-74.
15. Viswanathan AN, Beriwal S, De Los Santos JF, Demanes DJ, Gaffney D, Hansen J, et al. (2012) American Brachytherapy Society. American Brachytherapy Society consensus guidelines for locally advanced carcinoma of the cervix. Part II: high-dose-rate brachytherapy. *Brachytherapy*, **11**(1): 47-52.
16. Haie-Meder C, Pötter R, Van Limbergen E, Briot E, De Brabandere M, Dimopoulos J, et al. (2005) Gynaecological (GYN) GEC-ESTRO Working Group. Recommendations from Gynaecological (GYN) GEC-ESTRO Working Group (I): concepts and terms in 3D image based 3D treatment planning in cervix cancer brachytherapy with emphasis on MRI assessment of GTV and CTV. *Radiat Oncol*, **74**(3): 235-45.
17. Wu A, Ulin K, Sternick ES (1988) A dose homogeneity index for evaluating 192Ir interstitial breast implants. *Med Phys*, **15**(1): 104-7.
18. Major T, Polgár C, Fodor J, Somogyi A, Németh G (2002) Conformality and homogeneity of dose distributions in interstitial implants at idealized target volumes: a comparison between the Paris and dose-point optimized systems. *Radiat Oncol*, **62**(1): 103-11.
19. Fröhlich G, Geszti G, Vízkeleti J, Ágoston P, Polgár C, Major T. (2019) Dosimetric comparison of inverse optimisation methods versus forward optimisation in HDR brachytherapy of breast, cervical and prostate cancer. *Strahlenther Onkol*, **195**(11): 991-1000.
20. Chakrabarti B, Basu-Roy S, Kar SK, Das S, Lahiri A (2017) Comparison of dose volume parameters evaluated using three forward planning - optimization techniques in cervical cancer brachytherapy involving two applicators. *J Contemp Brachytherapy*, **9**(5): 431-445.
21. Jamema SV, Kirisits C, Mahantshetty U, Trnkova P, Deshpande DD, Shrivastava SK, et al. (2010) Comparison of DVH parameters and loading patterns of standard loading, manual and inverse optimization for intracavitary brachytherapy on a subset of tandem/ovoid cases. *Radiat Oncol*, **97**(3): 501-6.
22. Yoshio K, Murakami N, Morota M, Harada K, Kitaguchi M, Yamagishi K, et al. (2013) Inverse planning for combination of intracavitary and interstitial brachytherapy for locally advanced cervical cancer. *J Radiat Res*, **54**(6): 1146-52.
23. Kubicky CD, Yeh BM, Lessard E, Joe BN, Speight JL, Pouliot J, et al. (2008) Inverse planning simulated annealing for magnetic resonance imaging-based intracavitary high-dose-rate brachytherapy for cervical cancer. *Brachytherapy*, **7**(3): 242-7.
24. Kumar M, Thangaraj R, Alva RC, Koushik K, Ponni A, Achar JM (2019) Impact of different dose prescription schedules on EQD2 in high-dose-rate intracavitary brachytherapy of carcinoma cervix. *J Contemp Brachytherapy*, **11**(2): 189-193.